

Article

## A Combined Cooperative Braking Model with a Predictive Control Strategy in an Electric Vehicle

Hongqiang Guo, Hongwen He \* and Fengchun Sun

National Engineering Laboratory for Electric Vehicles, Beijing Institute of Technology, Beijing 100081, China; E-Mails: guohongqiang666@163.com (H.G.); sunfch@bit.edu.cn (F.S.)

\* Author to whom correspondence should be addressed; E-Mail: hwhebit@bit.edu.cn; Tel./Fax: +86-10-6891-4842.

Received: 11 October 2013; in revised form: 4 December 2013 / Accepted: 4 December 2013 /

Published: 13 December 2013

---

**Abstract:** Cooperative braking with regenerative braking and mechanical braking plays an important role in electric vehicles for energy-saving control. Based on the parallel and the series cooperative braking models, a combined model with a predictive control strategy to get a better cooperative braking performance is presented. The balance problem between the maximum regenerative energy recovery efficiency and the optimum braking stability is solved through an off-line process optimization stream with the collaborative optimization algorithm (CO). To carry out the process optimization stream, the optimal Latin hypercube design (Opt LHD) is presented to discrete the continuous design space. To solve the poor real-time problem of the optimization, a high-precision predictive model based on the off-line optimization data of the combined model is built, and a predictive control strategy is proposed and verified through simulation. The simulation results demonstrate that the predictive control strategy and the combined model are reasonable and effective.

**Keywords:** electric vehicles; cooperative braking; combined model; collaborative optimization algorithm; predictive control strategy

### Nomenclature:

ABS	Anti-lock braking system
ASA	Adaptive simulated annealing
CO	Collaborative optimization algorithm
EV	Electric vehicle
Opt LHD	The optimal Latin hypercube design

$SoC$	The state of charge
$R^2$	Multiple correlation coefficient
$v$	The vehicle speed
$T_{m1}$	The front motor regenerative braking torque
$T_{m2}$	The rear motor regenerative braking torque
$T_{hf}$	The front hydraulic braking torque
$T_{hr}$	The rear hydraulic braking torque
$F_{xb1}$	The front road braking force
$F_{xb2}$	The rear road braking force
$F_{z1}$	The road normal reaction force in the front wheels
$F_{z2}$	The road normal reaction force in the rear wheels
$r_w$	The radius of the wheels
$\omega_f$	The angular velocity of the front wheels
$\omega_r$	The angular velocity of the rear wheels
$N_{xf}$	The thrust of the front axle
$N_{xr}$	The thrust of the rear axle
$m_f g$	The gravity of the front axle
$m_r g$	The gravity of the rear axle
$G$	The mass of the vehicle
$L_f$	The front wheelbase
$L_r$	The rear wheelbase
$L$	The wheelbase
$H_g$	The centroid height of the vehicle
$T_{rm}$	The required braking torque
$z$	The braking severity
$m$	The mass of the vehicle
$\beta$	The braking force distribution coefficient
$T_m$	The total regenerative braking torque
$\alpha$	The coordinate distribution coefficient
$\eta$	The coordinate coefficient of the hydraulic brakes
$\rho$	The performance value of the proportional valve
$\gamma$	The secondary allocation coefficient
$T_{opt}$	The ideal regenerative braking torque
$T_{mot \text{ generation}}$	The maximum charge torque of motors
$T_{bat \text{ charge}}$	The maximum rechargeable torque of the battery
$n$	The motor speed
$I_c$	The charging current
$f_T(n)$	The charging torque of motors
$f_{\text{efficient}}(n, f_T(n))$	The charging efficiency of the motors
$f_T(SoC, n)$	The rechargeable torque of the battery
$P_{\text{charging}}$	The charging power
$P_{\text{charging max}}$	The maximum charging power

$f_{\text{efficient}}(SoC, I_c)$	The rechargeable torque efficiency of the battery
$E_{soc}$	The voltage of the battery
$R$	The internal resistance of battery
$\mu_f$	The adhesion rate of the front wheels
$\mu_r$	The adhesion rate of the rear wheels
$\beta_{\text{opt}}$	The optimum braking stability value
$T_{\text{out1}}$	The maximum braking torque of the Motor 1 under a given $n$
$T_{\text{out2}}$	The maximum braking torque of the Motor 2 under a given $n$
$\beta$ -lower	The lower bound of $\beta$
$\beta$ -upper	The upper bound of $\beta$
$T_{\text{road front}}$	The maximum road braking torque of the front wheels
$T_{\text{road rear}}$	The maximum road braking torque of the rear wheels
$\varepsilon$	the evaluation parameter of $T_m$
$\mu$	The relative error of $\alpha$
$\tau$	The relative error of $\gamma$
$\tilde{\alpha}$	The predictive value of $\alpha$
$\tilde{\gamma}$	The predictive value of $\gamma$
$\tilde{\beta}$	The predictive value of $\beta$
$\tilde{T}_{hf}$	the predictive value of $T_{hf}$
$\tilde{T}_{hr}$	The predictive value of $T_{hr}$
$\tilde{T}_{m1}$	The predictive value of $T_{m1}$
$\tilde{T}_{m2}$	The predictive value of $T_{m2}$
$\zeta$	The evaluation parameter of $SoC$
$SoC_{\text{end}}$	The end-state of $SoC$
$SoC_{\text{initial}}$	The initial-state of $SoC$

## 1. Introduction

Oil crises have made energy a hot topic of discussion. Transportation consumes a large proportion of energy, and the application of electric vehicles (EVs) has become a global strategy for saving energy and using sustainable energy [1–3]. In order to improve the energy efficiency further, regenerative braking and mechanical braking cooperative systems are widely used in EVs. The regenerative electric energy can be stored in electric buffers, *i.e.*, batteries or capacitors and then in return power the vehicle [4]. The cooperative braking system can be classified into series and parallel types [5]. The series type can simultaneously coordinate regenerative and hydraulic brakes, and give better cooperative braking performance, but the whole braking system should be redeveloped. As the parallel type doesn't intervene in the hydraulic brakes, and the regenerative braking directly enforces the hydraulic braking, only a little development work is needed to meet the requirements, but the total braking force will possibly be greater than the total required braking force, to maintain the braking stability, the regenerative energy

recovery efficiency may be greatly limited [6]. It is worthy to research and find a solution to maximize the regenerative energy efficiency with not much development work needed.

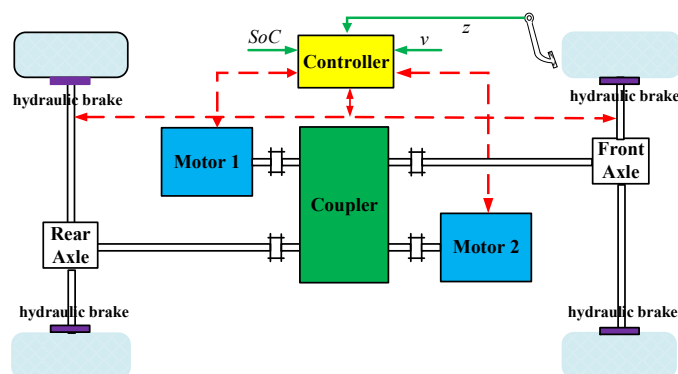
In the field of cooperative braking control, two kinds of braking scenarios are commonly studied. One is the emergency braking process, in which an integrated anti-lock braking system (ABS) with a motor regenerative braking is widely used [7–9]. The other is the normal deceleration process, with the aim of improving the regeneration energy efficiency and the coordinated control between the motor regenerative braking and the hydraulic brakes [10]. The control strategies for this case can be divided into two kinds: *i.e.*, the logic-threshold strategy and the ideal braking force distribution control strategy. For logic-threshold strategy, the control thresholds are usually determined after considering the maximum rechargeable capacity, tire-road friction condition, braking stability limitation and required braking severity and so on. For the braking stability is usually considered as a constraint, it is difficult to simultaneously maintain the braking stability and the optimum regenerative energy recovery efficiency [11–19]. For the ideal braking force distribution control strategy, the braking force follows the ideal braking force distribution curve (*I* curve), which makes the vehicle realize a better braking performance. The basic control principle can be expressed as follows: if the motor regenerative braking force meets the control strategy, the total braking force is provided only by the motor regenerative braking force; otherwise, the total braking force will be provided by motor regenerative braking and hydraulic brakes simultaneously. With respect to the series type, it can offer good cooperative braking performance. However, with respect to the parallel type, due to its over-reliance on the *I* curve, the regenerative energy recovery efficiency may be greatly limited [20–22].

In this paper, we only focus on the normal deceleration process. A combined cooperative braking model is proposed. With respect to the control strategy, differing from the tradition strategies, firstly two disciplines of the maximum regenerative energy recovery efficiency and the optimum braking stability are defined and an off-line optimization data is obtained by an off-line optimization stream. Then based on the off-line optimization data, a predictive model by Kriging method is obtained. Finally, a predictive control strategy is presented to solve the poor real-time problem of optimization, and the predictive control strategy is verified in a dynamic simulation.

## 2. Cooperative Braking System in an EV

As shown in Figure 1, the EV powertrain is a four-wheel drive system with two motors and a two-speed mechanical coupler.

**Figure 1.** The scheme of the cooperative braking system. *SoC*: the state of charge.

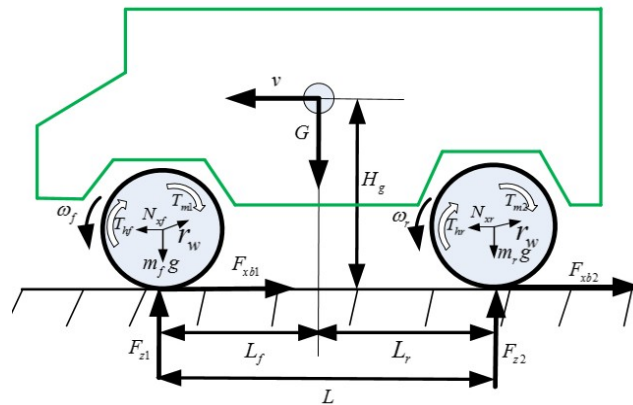


During cooperative braking, the two motors and the hydraulic brakes provide braking forces simultaneously to the front and rear axles. In our study, it's assumed that the road is a dry pavement that is able to provide enough adhesive force. Since only the normal deceleration process is studied, the braking severity is controlled within the range from 0 to 0.4 [23]. Additionally, due to the speed ratio restriction of the two-speed mechanical coupler which is 1.442, the lowest vehicle speed for cooperative braking is limited to 20 km/h.

### 3. Cooperative Braking Mathematic Models

A force analysis scheme on the wheels is shown in Figure 2, based on which three general cooperative braking mathematic models can be obtained.

**Figure 2.** The force analysis scheme.



#### 3.1. General Cooperative Braking Mathematic Models

##### 3.1.1. The Series Model

The series model should ensure that the total output braking torques equal to the required braking torque, which can be expressed as follows:

$$T_{m1} + T_{hf} + T_{m2} + T_{hr} = T_{rm} \tag{1}$$

where  $T_{rm}$  can be expressed as  $T_{rm} = mgr_w z$  and it is a known variable under a given  $z$ .

The braking force distribution coefficient is defined as the coefficient of the braking force of the front wheels divided by the whole braking force, which can be expressed by braking torques:

$$\frac{T_{m1} + T_{hf}}{T_{m1} + T_{hf} + T_{m2} + T_{hr}} = \beta \tag{2}$$

The total regenerative braking torque will be provided by the two motors, and the two motors should coordinate themselves to meet the optimization requirements:

$$T_{m1} + T_{m2} = T_m \tag{3}$$

$$\frac{T_{m1}}{T_{m1} + T_{m2}} = \alpha \tag{4}$$

where  $\alpha$  is controlled within the range from 0 to 1.

For the series model, the coordination between hydraulic brakes is another important requirement:

$$\frac{T_{hf}}{T_{hf} + T_{hr}} = \eta \tag{5}$$

where  $\eta$  is defined from 0 to 1.

Combining Equations (1)–(5) gives:

$$\begin{cases} T_m = \left(\frac{\beta - \eta}{\alpha - \eta}\right) T_{rm} \\ T_{m1} = \alpha \left(\frac{\beta - \eta}{\alpha - \eta}\right) T_{rm} \\ T_{m2} = (1 - \alpha) \left(\frac{\beta - \eta}{\alpha - \eta}\right) T_{rm} \\ T_{hf} = \eta \frac{(\alpha - \beta)}{(\alpha - \eta)} T_{rm} \\ T_{hr} = (1 - \eta) \frac{(\alpha - \beta)}{(\alpha - \eta)} T_{rm} \end{cases} \tag{6}$$

### 3.1.2. The Parallel Model

The parallel model needn't to coordinate the motors and the hydraulic brakes, and the hydraulic braking torques always follows the required braking torque. Therefore, Equation (1) can be rewritten as follows:

$$T_{hf} + T_{hr} = T_{rm} \tag{7}$$

No coordination between hydraulic brakes and the hydraulic braking torques should be based on the performance value of the proportional valve which is a constant value when braking severity lower than 0.4:

$$T_{hf} = \rho T_{hr} \tag{8}$$

Other equations will be the same as the series model. Combining Equations (2)–(4), (7) and (8), we can get:

$$\begin{cases} T_m = \frac{(\rho\beta + \beta - \rho)}{(\alpha - \beta)(1 + \rho)} T_{rm} \\ T_{m1} = \frac{\alpha(\rho\beta + \beta - \rho)}{(\alpha - \beta)(1 + \rho)} T_{rm} \\ T_{m2} = \frac{(1 - \alpha)(\rho\beta + \beta - \rho)}{(\alpha - \beta)(1 + \rho)} T_{rm} \\ T_{hf} = \frac{\rho T_{rm}}{(1 + \rho)} \\ T_{hr} = \frac{T_{rm}}{(1 + \rho)} \end{cases} \tag{9}$$

### 3.1.3. The Combined Model

Reallocating the required braking severity between motors and hydraulic brakes by a secondary allocation coefficient is the basic principle of the combined model. Most noteworthy is that the current parallel braking system doesn't need reforming considerably. The hydraulic braking torques are still in accordance with the performance of the proportional valve, the only difference is that its assigned braking severity is a part of the whole braking severity, and the other braking severity will be allocated to the motors.

Equations (1)–(4) in the series model and Equation (8) in the parallel model will be used to make up a combined model. Then  $T_m$ ,  $T_{m1}$ ,  $T_{m2}$ ,  $T_{hf}$  and  $T_{hr}$  can be realized as follows:

$$\begin{cases} T_m = \frac{T_{rm}[\rho - \beta(1 + \rho)]}{\rho - \rho\alpha - \alpha} \\ T_{m1} = \frac{T_{rm}\alpha[\rho - \beta(1 + \rho)]}{\rho - \rho\alpha - \alpha} \\ T_{m2} = \frac{T_{rm}(1 - \alpha)[\rho - \beta(1 + \rho)]}{\rho - \rho\alpha - \alpha} \\ T_{hf} = \frac{T_{rm}\rho(\alpha - \beta)}{(\alpha - \rho + \alpha\rho)} \\ T_{hr} = \frac{T_{rm}(\alpha - \beta)}{(\alpha - \rho + \alpha\rho)} \end{cases} \quad (10)$$

The secondary allocation coefficient is defined as the ratio of the required braking torque divided by the total regenerative braking torque:

$$\gamma = \frac{\rho - \beta - \beta\rho}{\rho - \rho\alpha - \alpha} \quad (11)$$

## 3.2. Optimization Cooperative Braking Mathematic Models

### 3.2.1. The Ideal Regenerative Energy Recovery Efficiency Objective

Generally, the regenerative energy recovery capability is limited by the battery and the motors simultaneously. Additionally, the efficiency of the battery and the motors also considerably affects the regenerative energy recovery efficiency. Regenerative energy recovery strategy should consider the both factors. In this study, the regenerative braking capacity is described by braking torque. The ideal regenerative braking torque is defined as follows:

$$T_{opt} = \min(T_{mot\_generation}, T_{bat\_charge}) \quad (12)$$

where  $T_{mot\_generation}$  and  $T_{bat\_charge}$  can be obtained by Equations (13) and (14), respectively:

$$T_{mot\_generation} = f_T(n)f_{efficient}(n, f_T(n)) \quad (13)$$

$$T_{bat\_charge} = f_T(SoC, n)f_{efficient}(SoC, I_c) \quad (14)$$

where  $f_T(n)$  can be obtained by the relationship table of  $n$  vs.  $f_T(n)$  through interpolation method;  $f_{efficient}(n, f_T(n))$  can be obtained by the relationship table of  $n, f_T(n)$  vs.  $f_{efficient}(n, f_T(n))$  through interpolation method; and  $f_T(SoC, n)$  can be obtained by Equation (15) which is shown below.

Firstly, according to *SoC*, the charging power can be expressed as follows:

$$\begin{aligned}
 & \text{if } SoC < 0.3 \\
 & \quad P_{charging} = P_{charging\_max} \\
 & \text{elseif } 0.3 < SoC < 0.8 \\
 & \quad P_{charging} = \frac{0.8 - SoC}{0.5} P_{charging\_max} \\
 & \text{elseif } SoC > 0.8 \\
 & \quad P_{charging} = 0 \\
 & \quad \text{end} \\
 & \text{end} \\
 & \text{end}
 \end{aligned}$$

Then the charging torque can be expressed as follows:

$$f_T(SoC, n) = \frac{9550 P_{charging}}{n} \tag{15}$$

With regard to  $f_{efficient}(SoC, I_c)$ , it is mainly subjected to  $I_c$  and *SoC*. According to the relationship curve of  $I_c$  vs. charging efficient and the relationship curve of *SoC* vs. charging efficient under a constant temperature of battery,  $f_{efficient}(SoC, I_c)$  can be obtained by interpolation method.

The charging current of battery can be deduced by Equation (16):

$$p_{charging} = (E_{soc} - I_c R) I_c \tag{16}$$

where  $E_{SoC}$  can be obtained by the relationship curve of *SoC* vs.  $E_{SoC}$  through the interpolation method; and  $R$  can be obtained by the relationship of *SoC* vs.  $R$  through the interpolation method.

### 3.2.2. The Ideal Braking Stability Objective

Generally, if the adhesion rates between front and rear wheels are equal in every braking severity, the vehicle will make the maximum utilization of adhesion coefficient, and the optimum braking stability will also be reached [20]. Based on the force analysis scheme in Figure 2 and reference [23], the ideal braking force distribution condition can be expressed as follows:

$$\mu_f = \mu_r \tag{17}$$

According to the definition of  $\mu_f$  and  $\mu_r$ , we can get:

$$\begin{cases} \mu_f = \frac{F_{xb1}}{F_{z1}} \\ \mu_r = \frac{F_{xb2}}{F_{z2}} \end{cases} \tag{18}$$

Substituting Equation (18) into Equation (17), an equilibrium equation can be obtained as follows:

$$\frac{F_{xb1}}{F_{z1}} = \frac{F_{xb2}}{F_{z2}} \tag{19}$$

To get the expression of  $\beta$ , Equation (19) can be realized as follows:

$$\frac{F_{xb1}}{F_{xb1} + F_{xb2}} = \frac{F_{z1}}{F_{z1} + F_{z2}} \tag{20}$$

Then, we can get:

$$\beta = \frac{F_{z1}}{F_{z1} + F_{z2}} \tag{21}$$

According to the braking theory,  $F_{z1}$  and  $F_{z2}$  can be expressed as follows:

$$\begin{cases} F_{z1} = \frac{G}{L}(L_r + zH_g) \\ F_{z2} = \frac{G}{L}(L_f - zH_g) \end{cases} \tag{22}$$

Substituting Equation (22) into Equation (21), the ideal braking force distribution value which is also the optimum braking stability objective value can be realized as follows:

$$\beta_{opt} = \frac{L_r + zH_g}{L} \tag{23}$$

With regard to  $I$  curve, it can be plotted by  $z$  as the horizontal axis and  $\beta_{opt}$  as the vertical axis.

### 3.3. Boundary Conditions

#### 3.3.1. Regenerative Braking Stability Scope Constraints

Generally, the adhesion rate of the front wheels being bigger than or equal to the rear wheels is the precondition for the braking stability [23]. Therefore, the braking stability condition can be expressed by Inequality Equation (24):

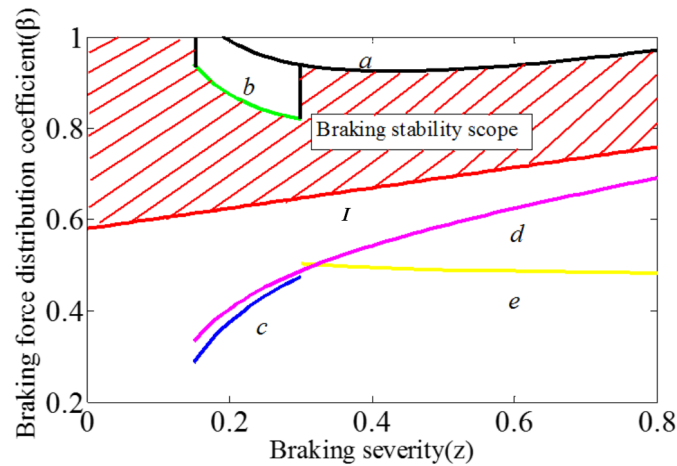
$$\beta \geq \beta_{opt} = \frac{L_r + zH_g}{L}; \quad 0 \leq z \leq 0.8 \tag{24}$$

Additionally, the braking regulations also should be followed. In this paper, the braking regulation of the ZBT 24007-1989 can be expressed as follows:

$$\begin{cases} \beta \geq \frac{L_r + zH_g}{L}; & 0 \leq z \leq 0.3 \\ \frac{(z - 0.08)(L_r + zH_g)}{zL} < \beta \leq \frac{(z + 0.08)(L_r + zH_g)}{zL}; & 0.15 \leq z \leq 0.3 \\ \beta \geq 1 - \frac{(z + 0.25)L}{0.74(L_f - zH_g)z}; & 0.3 \leq z \leq 0.8 \\ 1 - \frac{(L_f - zH_g)(\frac{z - 0.1}{0.85} + 0.2)}{Lz} \leq \beta \leq \frac{(L_r + zH_g)(\frac{z - 0.1}{0.85} + 0.2)}{Lz}; & 0.2 \leq z \leq 0.8 \end{cases} \tag{25}$$

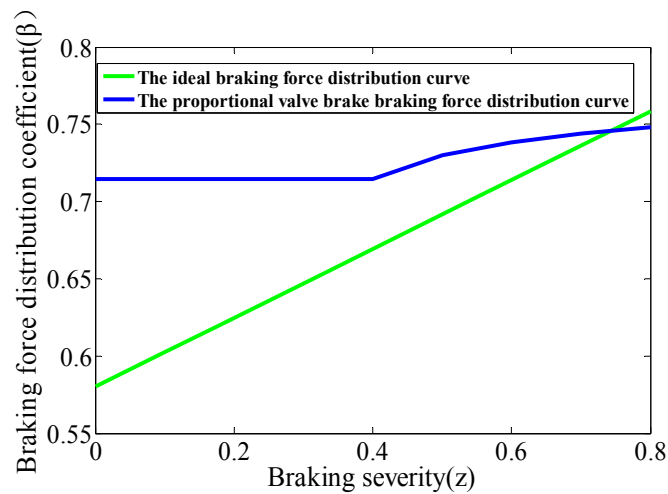
Based on Inequality Equation (24) and Inequality Equation (25), the braking stability scope can be plotted in Figure 3, where  $a$ ,  $b$ ,  $c$ ,  $d$  and  $e$  are the limit curves of the ZBT 24007-1989; and  $I$  is the ideal braking force distribution curve which is also the lower limit curve of the braking stability. The shadow scope is the ultimate braking stability scope. In off-line optimization and dynamic simulation, the lower bound is denoted by  $\beta$ -lower, and the upper bound is denoted by  $\beta$ -upper in this paper.

Figure 3. The braking stability scope.



Additionally, the vehicle is equipped with a proportional valve, for the combined model and the parallel model, during cooperative braking decelerate, the hydraulic brakes will follow the performance of the proportional valve in Figure 4.

Figure 4. The proportional valve performance.



### 3.3.2. Constraints According to the Mathematic Models

For each model,  $T_m > 0$  is the primary constraint. According to the expressions of  $T_m$  in the three models, Inequalities Equation (26) can be obtained as follows:

$$\begin{cases} T_m = \left( \frac{\beta - \eta}{\alpha - \eta} \right) T_{rm} \geq 0 & \text{The series model} \\ T_m = \frac{(\rho\beta + \beta - \rho)}{(\alpha - \beta)(1 + \rho)} T_{rm} \geq 0 & \text{The parallel model} \\ T_m = \frac{T_{rm} [\rho - \beta(1 + \rho)]}{\rho - \rho\alpha - \alpha} \geq 0 & \text{The combined model} \end{cases} \quad (26)$$

Based on the Inequalities Equation (26) and the braking stability scope which is shown in Figure 3, the constraints of  $\beta$ ,  $\alpha$  and  $\eta$  can be expressed as follows:

With the series model:

$$\begin{array}{ll} \text{Case 1} & \begin{cases} \beta_{opt} \leq \beta < \eta \\ 0 \leq \alpha < \eta \end{cases} & \text{Case 2} & \begin{cases} \beta > \eta \ \& \ \beta \in \text{braking stability scope} \\ 1 \geq \alpha > \eta \end{cases} \end{array}$$

With the parallel model:

$$\begin{array}{ll} \text{Case 1} & \begin{cases} \beta_{opt} \leq \beta < \frac{\rho}{\rho+1} \\ 0 \leq \alpha < \beta \end{cases} & \text{Case 2} & \begin{cases} \beta > \frac{\rho}{\rho+1} \ \& \ \beta \in \text{braking stability scope} \\ 1 \geq \alpha > \beta \end{cases} \end{array}$$

With the combined model:

$$\begin{array}{ll} \text{Case 1} & \begin{cases} \beta_{opt} \leq \beta < \frac{\rho}{\rho+1} \\ 0 \leq \alpha < \frac{\rho}{\rho+1} \end{cases} & \text{Case 2} & \begin{cases} \beta > \frac{\rho}{\rho+1} \ \& \ \beta \in \text{braking stability scope} \\ 1 \geq \alpha > \frac{\rho}{\rho+1} \end{cases} \end{array}$$

Generally, the nearer  $\beta$  is to the  $\beta_{opt}$ , the better braking stability will be. Therefore, Case1 is the best choice for each model in optimization.

### 3.3.3. Other Constraints

- (1) The total regenerative braking torque should be lower than the ideal regenerative braking torque which means:  $T_m \leq T_{opt}$ .
- (2) For each motor, the regenerative braking torque should be lower than the maximum braking torque of each motor under a given motor speed, which means:  $T_{m1} \leq T_{out1}$  and  $T_{m2} \leq T_{out2}$ .
- (3) The total braking torque of the wheels should be lower than the maximum road braking torque:

$$\begin{cases} T_{m1} + T_{hf} \leq T_{road\_front} \\ T_{m2} + T_{hr} \leq T_{road\_rear} \end{cases} \tag{27}$$

### 3.3.4. Two Disciplines of the Cooperative Braking System

To optimize the cooperative braking performance, two disciplines are established as follows:

$$\min \quad f_1 = \left( \frac{T_m - T_{opt}}{T_{opt}} \right)^2 \tag{28}$$

$$\min \quad f_2 = \left( \frac{\beta - \beta_{opt}}{\beta_{opt}} \right) \tag{29}$$

where Equation (28) is the maximum regenerative energy recovery efficiency discipline; and Equation (29) is the optimum braking stability discipline.

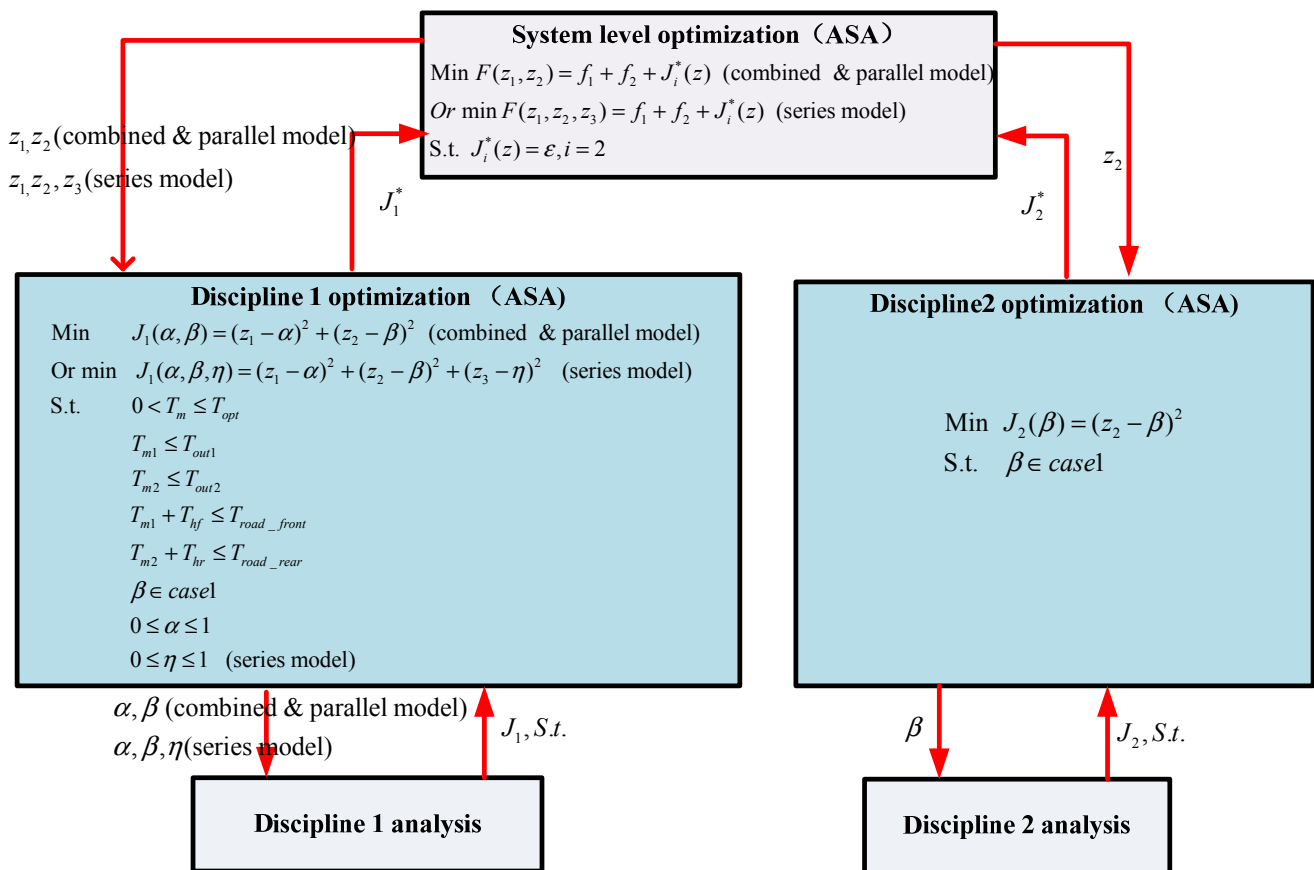
### 3.3.5. Collaborative Optimization Algorithm

Two disciplines have the same variable  $\beta$  according to Equations (28) and (29) and the expression of  $T_m$ . If  $\beta$  changes, two disciplines will change simultaneously, whether they will reach an optimum state at the same time is a key point in this study. In addition, complicated constraints are introduced in

the optimization. Collaborative optimization algorithm (CO), of which the basic theory refers to [24], has a greater advantage to solve them.

Figure 5 shows the collaborative optimization algorithm of the cooperative braking system, where  $z_1, z_2$  and  $z_3$  are the system variables and denote the discipline variable  $\alpha, \beta$  and  $\eta$ , respectively. To carry out the collaborative optimization algorithm, adaptive simulated annealing (ASA) is adopted in this study. ASA was put forward by Ingber [25] in 1992, and has the advantages of quick convergence speed, low requirements for initial conditions, and better identification of local optimal solutions, etc.

Figure 5. The collaborative optimization algorithm.



### 3.4. Off-Line Process Optimization Design

#### 3.4.1. Discrete Design Space

Generally, the vehicle speed  $v$ , the battery  $SoC$  and the braking severity  $z$  constitute the input design space of the cooperative braking system, and the vehicle can be broken at any design point. Therefore, the input design space is a continuous space. To carry out an off-line optimization stream, and set up a predictive model, the continuous space should be discretized. In this paper, the optimal Latin hypercube design (Opt LHD) is reasonable for it, which has better space-filling performance and better uniform than other designs of experiment. The continuous space is defined as follows:

$$\begin{cases} SoC \in (0.1 - 0.8) \\ v \in (20 - 100) \text{ km/h} \\ z \in (0.01 - 0.4) \end{cases}$$

The discrete sample points are listed in Table 1.

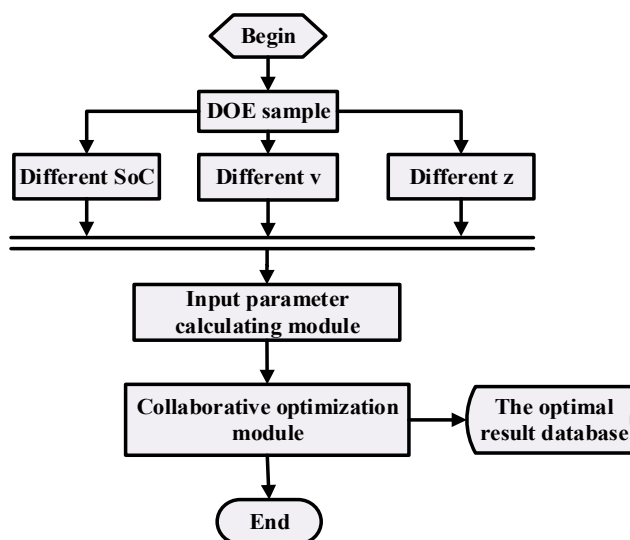
**Table 1.** The discrete sampling points.

Sampling points	SoC	v (km/h)	z
1	0.35526	89.51	0.35862
2	0.23754	47.868	0.24502
3	0.51622	98.318	0.15679
4	0.5967	62.362	0.3512
.	.	.	.
.	.	.	.
.	.	.	.
617	0.58468	95.115	0.07207
618	0.35706	88.468	0.10057
619	0.55766	47.708	0.28874

### 3.4.2. Off-Line Process Optimization Stream

As shown in Figure 6, the input parameter calculating module can calculate the parameters of  $\beta_{opt}$ ,  $T_{opt}$ ,  $T_{out1}$ ,  $T_{out2}$ ,  $\beta$ -lower,  $\beta$ -upper and  $T_{rm}$  according to the DOE sample points in Table 1. Then the parameters are passed to the collaborative optimization module to carry out a collaborative optimization analysis. Finally, all the optimum results are stored in the optimal result database to make a predictive model.

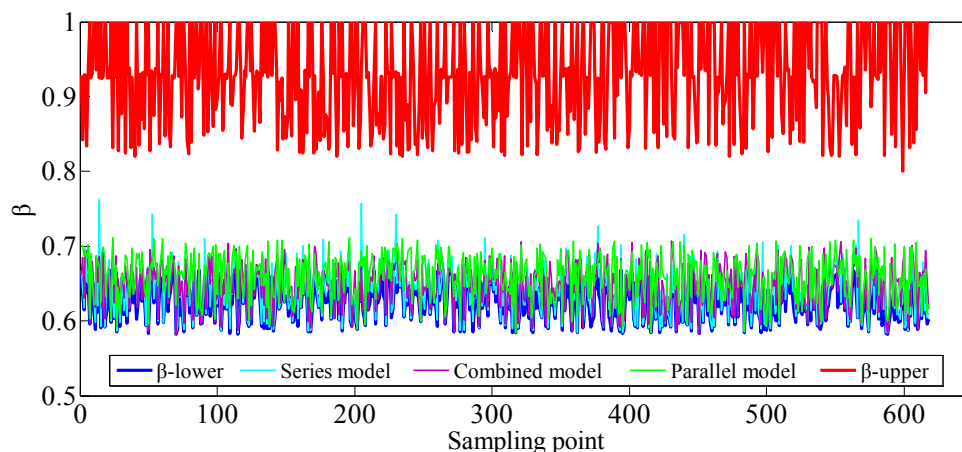
**Figure 6.** The off-line process optimization stream.



## 4. Optimization Results and Discussion

Figure 7 shows the braking force distribution coefficient ( $\beta$ ) of the three models, and three conclusions can be obtained from this figure. Firstly, for every model,  $\beta$  always falls into the braking stability scope. Secondly,  $\beta$  is close to  $\beta$ -lower ( $\beta_{opt}$ ), which means that all the models can make a perfect braking stability. Thirdly, since some optimization results offset the  $\beta_{opt}$  largely for the series model, the combined model and the parallel model have a better braking force distribution.

**Figure 7.** The braking force distribution coefficient.

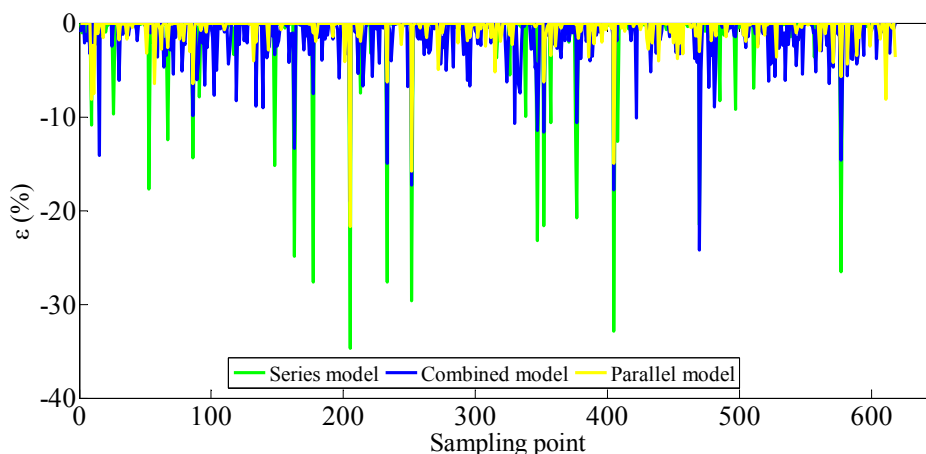


To evaluate the regenerative energy recovery efficiency of the three models, an evaluation parameter  $\varepsilon$  is defined as follows:

$$\varepsilon = \frac{T_m - T_{opt}}{T_{opt}} \times 100\% \tag{30}$$

Figure 8 shows the evaluation parameter  $\varepsilon$  in every sampling point of the three models. Generally speaking, the smaller  $\varepsilon$  is, the nearer  $T_m$  will be to  $T_{opt}$  and the better braking performance will be. In this perspective, the parallel model has a better performance, and the combined model takes a second place, while the series model makes the worst performance. Based on this, the parallel model is seemingly the best model, but a problem needs to be noticed that the regenerative energy recovery efficiency of it is based on an extra required braking force. Although it can ideally follow the ideal regenerative braking torque point, a braking instability problem may emerge. Therefore, taking into account the braking stability, the combined model and the series model may be better than the parallel model.

**Figure 8.** The evaluation parameter of  $\varepsilon$ .



Given the above analysis, the combined model not only has a better braking stability, but also can maximize the regenerative braking energy recovery efficiency compared to other models. Thus the combined model has a considerable application value.

### 5. Predictive Control Model and Dynamic Simulation Results

#### 5.1. Predictive Control Model

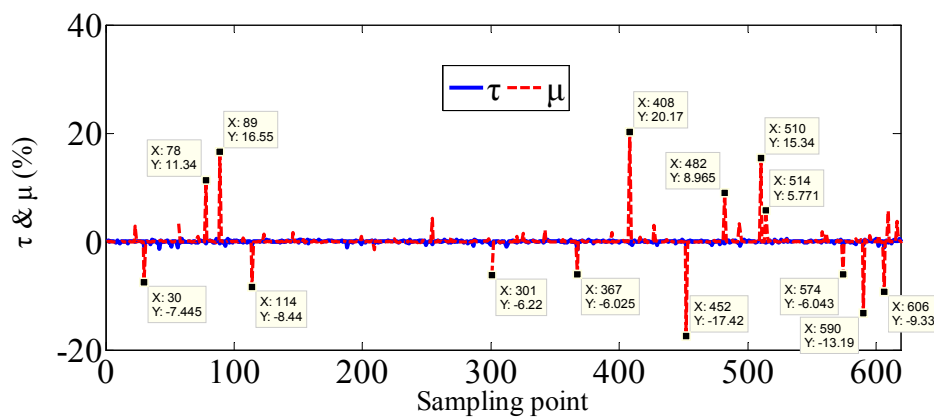
To carry out a dynamic simulation, a predictive model, which is established by the optimal result database, is proposed. The predictive model is also called the Kriging approximation model. It is a type of the interpolation technique, of which the basic theory was presented in reference [26]. The predictive model can be built through MATLAB. The accuracy of the predictive model is evaluated by the multiple correlation coefficient ( $R^2$ ). In this study, the  $R^2$  of  $\tilde{\alpha}$  and  $\tilde{\gamma}$  are 0.95939 and 0.98778, respectively.

To better evaluate the effectiveness of the predictive model, a relative error analysis is also carried out between the predictive values and the off-line optimization values. Define:

$$\begin{cases} \mu = \frac{\tilde{\alpha} - \alpha}{\alpha} \times 100\% \\ \tau = \frac{\tilde{\gamma} - \gamma}{\gamma} \times 100\% \end{cases} \quad (31)$$

It can be seen in Figure 9, with respect to  $\mu$ , 14 sampling points are beyond the expected error by 5%, and the maximum value is 20.17%. In braking process, the predictive error of them may cause unexpected results, which is not permitted. On the contrary, for  $\tau$ , it has fairly high prediction accuracy and all of the relative errors of the sampling points fall into the expected error scope.

Figure 9. The relative error analysis results.



Substituting the predictive model into Equation (10), a predictive control model can be obtained. Additionally, two additional conditions are also defined in the predictive control model to ensure braking safety. The additional conditions are defined as follows:

Condition 1: if  $\beta$  is lower than  $\beta_{opt}$ , which means the vehicle falls into the instability scope, then the motors will be cut off, and the whole braking torque will be offered only by hydraulic brakes.

Condition 2: if  $\beta$  is bigger than  $\beta_{opt}$ , which means the vehicle falls into the stability scope, yet for all that, any  $T_{m1}$  or  $T_{m2}$  may be bigger than the maximum motor braking torque, so the other additional condition should be considered. It can be described as follows: when  $T_{m1} > T_{out1}$  and  $T_{m2} > T_{out2}$ , make  $T_{m2} = T_{out2}$ , then,  $\beta$  may be bigger than the current value according to Equation (2), and the vehicle will still be broken safely based on the braking stability scope (Figure 3), however, the regenerative

braking energy recovery efficiency may be limited; when  $T_{m1} > T_{out1}$ ;  $T_{m2} \leq T_{out2}$  or  $T_{m1} > T_{out1}$ ;  $T_{m2} > T_{out2}$ , if make  $T_{m1} = T_{out1}$ ,  $\beta$  may be lower than the current value, and the vehicle may be broken unsafely, in which case, the vehicle will be broken according to Condition 1:

$$\left\{ \begin{array}{l} \tilde{\beta} = \frac{\rho - \tilde{\gamma}(\rho - \rho\tilde{\alpha} - \tilde{\alpha})}{(1 + \rho)} \\ \tilde{T}_{m1} = \frac{T_{rm}\tilde{\alpha}[\rho - \tilde{\beta}(1 + \rho)]}{\rho - \rho\tilde{\alpha} - \tilde{\alpha}} \\ \tilde{T}_{m2} = \frac{T_{rm}(1 - \tilde{\alpha})[\rho - \tilde{\beta}(1 + \rho)]}{\rho - \rho\tilde{\alpha} - \tilde{\alpha}} \text{ condition 1} \\ \tilde{T}_{hf} = \frac{T_{rm}\rho(\tilde{\alpha} - \tilde{\beta})}{(\tilde{\alpha} - \rho + \tilde{\alpha}\rho)} \\ \tilde{T}_{hr} = \frac{T_{rm}(\tilde{\alpha} - \tilde{\beta})}{(\tilde{\alpha} - \rho + \tilde{\alpha}\rho)} \end{array} \right. \left\{ \begin{array}{l} \text{If } \tilde{\beta} < \beta_{opt} \\ \tilde{T}_{m1} = 0; \\ \tilde{T}_{m2} = 0; \\ \tilde{T}_{hf} = \frac{\rho T_{rm}}{(1 + \rho)}; \text{ condition 2} \\ \tilde{T}_{hr} = \frac{T_{rm}}{(1 + \rho)}; \\ \text{end} \end{array} \right. \left\{ \begin{array}{l} \text{If } \tilde{\beta} \geq \beta_{opt} \\ \text{if } \tilde{T}_{m2} > T_{out2}, \tilde{T}_{m1} \leq T_{out1} \\ \tilde{T}_{m2} = T_{out1}; \\ \tilde{T}_{hf} = \frac{T_{rm}\rho(\tilde{\alpha} - \tilde{\beta})}{(\tilde{\alpha} - \rho + \tilde{\alpha}\rho)}; \\ \tilde{T}_{hr} = \frac{T_{rm}(\tilde{\alpha} - \tilde{\beta})}{(\tilde{\alpha} - \rho + \tilde{\alpha}\rho)}; \\ \text{else if } \tilde{T}_{m2} \leq T_{out2}, \tilde{T}_{m1} > T_{out1} \text{ or } \tilde{T}_{m2} > T_{out2}, \tilde{T}_{m1} > T_{out1} \\ \text{condition 1;} \\ \text{end} \\ \text{end} \\ \text{end} \end{array} \right. \quad (32)$$

5.2. Dynamic Simulation Results

To verify the predictive control strategy, a dynamic simulation model of the vehicle is set up in MATLAB/Simulink soft. Three simple braking processes are defined in Figures 10–14, where t0 is the sum of the reaction time, the brake harmony time and the half of the braking force rise time; t1, t2 and t3 denote three braking processes, respectively. Additionally, the initial vehicle speed is 84 km/h. To better evaluate the reliability of the predictive control strategy, three cases are also defined as follows:

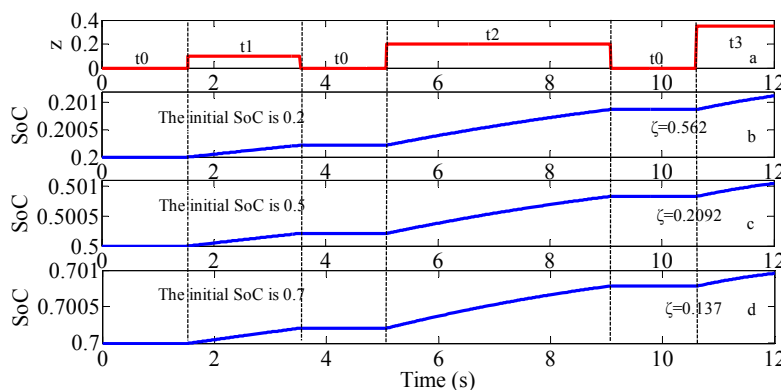
- (1) the initial battery SoC is 0.2;
- (2) the initial battery SoC is 0.5;
- (3) the initial battery SoC is 0.7.

Define:

$$\zeta = \frac{SoC_{end} - SoC_{initial}}{SoC_{initial}} \quad (33)$$

As shown in Figure 10, for the three cases, since the braking severity z is 0, during the braking time of t0, SoC will remain unchanged.

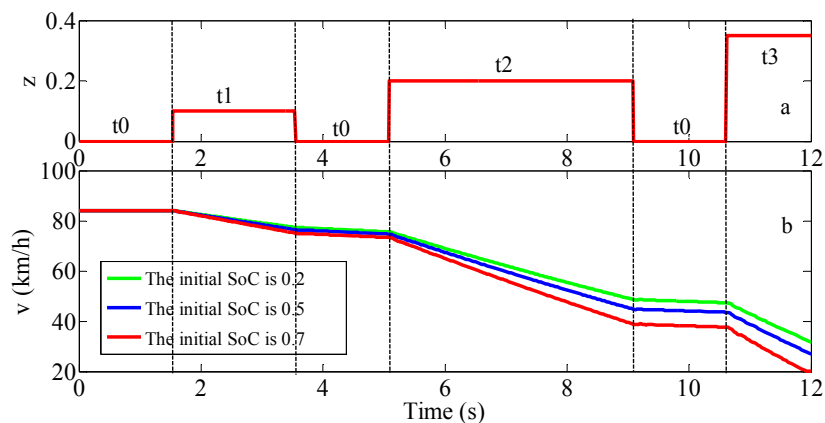
Figure 10. The simulation results of SoC.



During the braking time of  $t_1$ ,  $t_2$  and  $t_3$ ,  $SoC$  will increase linearly. Additionally, comparing the parameter of  $\zeta$  in the three cases, the smaller the initial  $SoC$  is, the bigger  $\zeta$  will be. The reason can be interpreted as follows: according to the charging performance of the battery, the lower  $SoC$  is, the more required charging torque will be, so when cooperative braking, more braking torque will be offered by motors and the increased  $SoC$  for the Case (1) will be bigger than other cases.

The simulation results of  $v$  in the three cases are shown in Figure 11. For any case, during the braking time of  $t_0$ , due to the braking severity  $z$  is 0,  $v$  will remain unchanged. During the braking time of  $t_1$ ,  $v$  will slow down linearly. During the braking time of  $t_2$ ,  $v$  continues slowing down. Since the braking severity  $z$  is bigger than the braking time of  $t_0$ , the slow-down slope is bigger than the braking time of  $t_1$ . Similarly, during the braking time of  $t_3$ , the slow-down tendency is the same as the above two cases, the only difference is that, the slow-down slope is the biggest. Additionally, comparing the three cases, it can be seen that, during the braking time of  $t_2$  and  $t_3$ , the slow-down tendencies of the three cases are different, which are caused by the predictive control model. For some cases, the predictive error may be bigger than the expected values, and then the additional conditions may be carried out. Therefore,  $T_{rm}$  will be limited and the slow-down slope will be different for the three cases.

**Figure 11.** The simulation results of  $v$ .



As shown in Figure 12, for each case, during the braking times of  $t_1$ ,  $t_2$  and  $t_3$ ,  $\beta$  is always close to  $\beta$ -lower, and falls into the braking stability scope. It means that the vehicle can maintain a better braking stability during braking deceleration.

**Figure 12.** The simulation results of  $\beta$ .

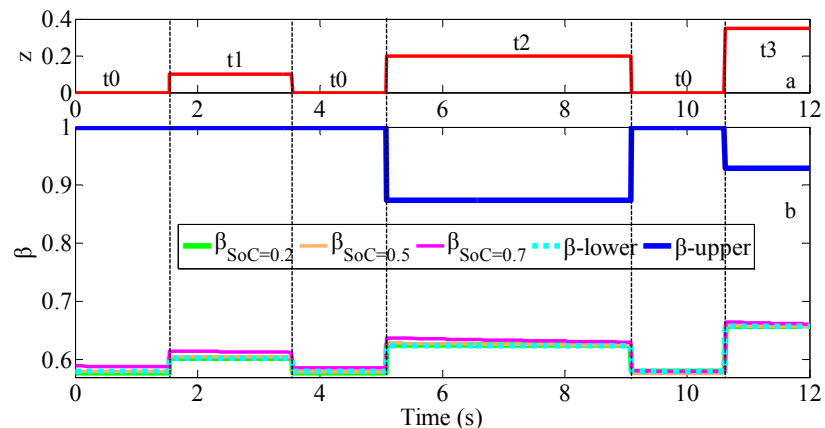
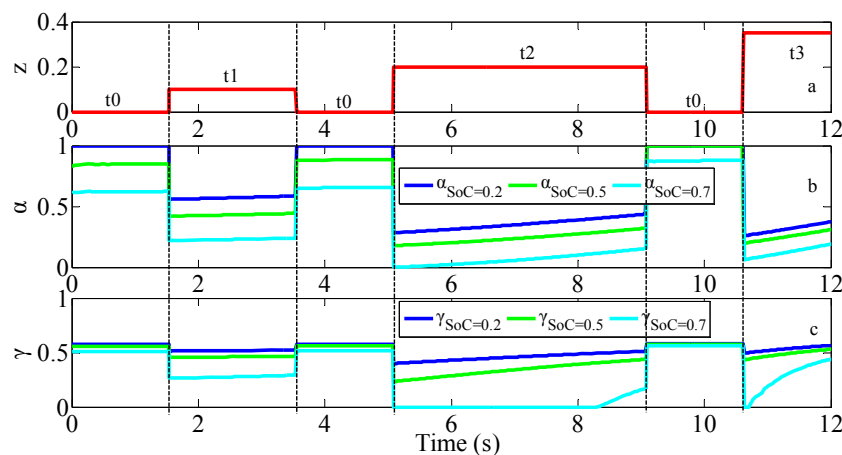
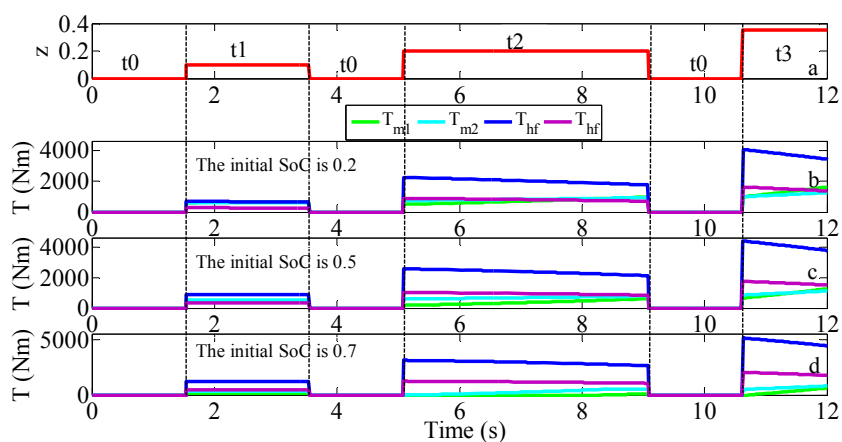


Figure 13 shows the changing trends of  $\alpha$  and  $\gamma$  in the three cases. Figure 14 shows the changing trends of  $T_{m1}$ ,  $T_{m2}$ ,  $T_{hf}$  and  $T_{hr}$ . Just as shown in Figure 13, during the braking time of  $t_0$ , theoretically speaking,  $\alpha$  and  $\gamma$  should be 0, however, the simulation results are just the opposite, and the reason can be explained that the braking severity predictive scope of the predictive model has been limited from 0.01 to 0.4, beyond this scope, the predictive value is unbelievable, nevertheless, owing to the  $T_{rm}$  expression, which is the first and foremost condition for the predictive model, the predictive values of  $T_{m1}$ ,  $T_{m2}$ ,  $T_{hf}$  and  $T_{hr}$  are 0 (Figure 13) which are meet the predictive requirement. During the braking time of  $t_1$ ,  $t_2$  and  $t_3$ ,  $\alpha$  will coordinate the two motors, and  $\gamma$  will also works which can reallocate the whole braking severity  $z$ . For the three cases, the bigger  $SoC$  is, the smaller  $\alpha$  and  $\gamma$  will be. With respect to  $\alpha$ , it means that the bigger  $SoC$  is, the smaller  $T_{m1}$  will be and more regenerative braking torque will be allocated to Motor 2. With regard to  $\gamma$ , it means that the bigger  $SoC$ , the smaller braking severity  $z$  will be allocated to the motors. Additionally, The values of  $\alpha$  and  $\gamma$  control the output braking torques of  $T_{m1}$ ,  $T_{m2}$ ,  $T_{hf}$  and  $T_{hr}$  which are shown in Figure 14.

**Figure 13.** The simulation results of  $\alpha$  and  $\gamma$ .



**Figure 14.** The simulation results of  $T$ .



## 6. Conclusions

A combined cooperative braking model with a predictive control strategy is proposed. The main concluding remarks are listed as follows:

- (1) A combined cooperative braking model was built and was evaluated by simulations. Compared to other models, the combined model is more reasonable for the cooperative braking system, which can provide a better braking stability under the condition that no additional braking torque is required for the braking system.
- (2) To get a tradeoff between the maximum regenerative energy recovery efficiency and the optimum braking stability, a CO is applied for the cooperative braking system.
- (3) To solve the poor real-time problem of the optimization, a high-precision predictive model based on the off-line optimization data of the combined model is built, and a predictive control strategy is proposed and verified through simulation. It can be seen that the predictive model can solve the poor real-time performance of the optimization. In addition, due to the predictive model is deduced by the off-line optimization results through the Kriging approximation method, it performs well with a good predictive precision for the cooperative braking system.
- (4) To avoid the possible conditions that the vehicle falls into a dangerous state in some cases due to the predictive precision of the predictive model, two additional conditions are provided to ensure braking safety, as a sacrifice, the cooperative braking performance will be limited.

To ensure the cooperative braking performance, a reliable prediction model for normal deceleration process and a control strategy for emergency braking process are vital to the cooperative braking system. Therefore, in our future work, considering the prediction errors, an uncertainty prediction model based on an uncertainty optimization results will be studied. Additionally, considering the braking safety problem in emergency braking process, a control strategy which is based on sliding mode control strategy and the combined model will also be researched.

### Conflicts of Interest

The authors declare no conflict of interest.

### References

1. Chau, K.; Li, W.; Lee, C. Challenges and opportunities of electric machines for renewable energy. *Prog. Electromagn. Res. B* **2012**, *42*, 45–74.
2. Abdelsalam, A.; Cui, S. A fuzzy logic global power management strategy for hybrid electric vehicles based on a permanent magnet electric variable transmission. *Energies* **2012**, *5*, 1175–1198.
3. Xiong, R.; He, H.; Sun, F.; Zhao, K. Online estimation of peak power capability of Li-batteries in electric vehicles by a hardware-in-loop approach. *Energies* **2012**, *5*, 1455–1469.
4. Falcone, P.; Khoshfetrat Pakazad, S.; Solyom, S. Predictive Approaches to Rear Axle Regenerative Braking control in Hybrid Vehicle. In Proceedings of the IEEE Conference on Decision and Control and 28th Chinese Control Conference, Shanghai, China, 16–18 December 2009; pp. 7627–7632.
5. Clikanek, S.; Bailey, K. Electric Vehicle Braking Systems. In Proceedings of the 14th International Electric Vehicle Symposium and Exhibition, Orlando, FL, USA, 15–17 December 1997.

6. Liang, B.; Lin, W. Optimal Regenerative Torque Control to Maximize Energy Recapture of Electric Vehicles. In Proceedings of the 2010 World Automation Congress, Kobe, Japan, 19–23 September 2010.
7. Bera, T.; Bhattacharya, K.; Samantaray, A. Bond graph model-based evaluation of a sliding mode controller for a combined regenerative and antilock braking system. *Proc. Inst. Mech. Eng. Part I J. Syst. Control Eng.* **2011**, *225*, 918–934.
8. Peng, D.; Zhang, Y.; Yin, C. Combined control of a regenerative braking and antilock braking system for hybrid electric vehicles. *Int. J. Automot. Technol.* **2008**, *9*, 749–757.
9. Zhang, J.; Chen, X.; Zhang, P. Integrated control of braking energy regeneration and pneumatic anti-lock braking. *Proc. Inst. Mech. Eng. Part D J. Automob. Eng.* **2010**, *224*, 587–610.
10. Zhang, J.; Lv, C.; Gou, J.; Kong, D. Cooperative control of regenerative braking and hydraulic braking of an electrified passenger car. *Proc. Inst. Mech. Eng. Part D J. Automob. Eng.* **2012**, *226*, 1289–1302.
11. Gao, Y.; Chen, L.; Ehsani, M. Investigation of the effectiveness of regenerative braking for EV and HEV. *SAE Trans.* **1999**, *108*, 3184–3190.
12. Bailey, K.E.; Cikanek, S.R. Comparison of Energy Recovery Capability of Electric Vehicle Braking Systems. In Proceedings of the 3th International Symposium on Advanced Vehicle Control, Aachen, Germany, 24–28 June 1996; Volume 2, pp. 1227–1252.
13. Jo, C.; Ko, J.; Yeo, H.; Yeo, T.; Hwang, S.; Kim, H. Cooperative regenerative braking control algorithm for an automatic-transmission-based hybrid electric vehicle during a downshift. *Proc. Inst. Mech. Eng. Part D J. Automob. Eng.* **2012**, *226*, 457–467.
14. Sangtarash, F.; Esfahanian, V.; Nehzati, H.; Haddadi, S.; Bavanpour, M.; Haghpanah, B. Effect of Different Regenerative Braking Strategies on Braking Performance and Fuel Economy in a Hybrid Electric Bus Employing CRUISE Vehicle Simulation. In Proceedings of the SAE International Powertrains, Fuels and Lubricants Congress, Shanghai, China, 23–25 June 2008.
15. Hoon, Y.; Hyunsoo, K. Development of Regenerative Braking Hydraulic Module and HIL Simulator for Hybrid Electric Vehicle. In Proceedings of the 23rd Chinese Control Conference, Wuxi, China, 10–13 August 2004; pp. 1551–1556.
16. Yeo, H.; Kim, T.; Kim, C.; Kim, H. Performance Analysis of Regenerative Braking System for Parallel Hybrid Electric Vehicle Using HILS. In Proceedings of the 14th International Electric Vehicle Symposium and Exhibition, Orlando, FL, USA, 15–17 December 1997.
17. Yeo, H.; Kim, H. Hardware-in-the-loop simulation of regenerative braking for a hybrid electric vehicle. *Proc. Inst. Mech. Eng. Part D J. Automob. Eng.* **2002**, *216*, 855–864.
18. Yao, J.; Zhong, Z.; Sun, Z. A Fuzzy Logic Based Regenerative Braking Regulation for a Fuel Cell Bus. In Proceedings of the IEEE International Conference on Vehicular Electronics and Safety (ICVES), Beijing, China, 13–15 December 2006; pp. 22–25.
19. Nabi, A.; Fazeli, A.; Valizadeh, M. Development of a Brake Control System for a Series Hybrid Electric City Bus Using Fuzzy Logic. In Proceedings of the IEEE International Conference on Mechatronics and Automation, Henan, China, 25–28 June 2006; pp. 1345–1350.
20. Ahn, J.; Jung, K.; Kim, D. Modeling and Simulation of Electro-Mechanical Brake for Hybrid Electric Vehicles. In Proceedings of the 22th International Electric Vehicle Symposium and Exhibition, Yokohama, Japan, 23–28 October 2006; pp. 687–697.

21. Jo, C.; Kim, H. Performance Analysis of Electro-Mechanical Brake System for a Hybrid Electric Vehicle Using HILS. In Proceedings of the 23th International Electric Vehicle Symposium and Exhibition, Anaheim, CA, USA, 2–5 December 2007; pp. 979–988.
22. Yeo, H.; Hwang, S.; Kim, H. Regenerative braking algorithm for a hybrid electric vehicle with CVT ratio control. *Proc. Inst. Mech. Eng. Part D J. Automob. Eng.* **2006**, *220*, 1589–1600.
23. Mitschke, M.; Wallentowitz, H. *Vehicle Dynamics* (in Chinese), 4th ed; Tsinghua University Press: Beijing, China, 2009; pp. 156–210; translated by Chen, M., Yu, Q.
24. Kroo, I.; Manning, V. Collaborative Optimization: Status and Directions. In Proceedings of the 8th AIAA/NASA/ISSMO Symposium on Multidisciplinary Analysis and Optimization, Long Beach, CA, USA, 6–8 September 2000.
25. Ingber, L. Adaptive simulated annealing (ASA): Lessons learned. *Control Cybern.* **1996**, *25*, 33–54.
26. Koch, P.; Wujek, B.; Golovidov, O.; Simpson, T. Facilitating Probabilistic Multidisciplinary Design Optimization Using Kriging Approximation Models. In Proceedings of the 9th AIAA/ISSMO Symposium on Multidisciplinary Analysis & Optimization, Atlanta, GA, USA, 4–6 September 2002.

© 2013 by the authors; licensee MDPI, Basel, Switzerland. This article is an open access article distributed under the terms and conditions of the Creative Commons Attribution license (<http://creativecommons.org/licenses/by/3.0/>).